

# Fence-Line Spectroscopic Measurements Suggest Carry-Over of Salt-Laden Aerosols into Flare Systems Is Common

Zachary R. Milani, Bradley M. Conrad, Cameron S. Roth, and Matthew R. Johnson\*



Cite This: *Environ. Sci. Technol. Lett.* 2023, 10, 1068–1074



Read Online

ACCESS |



Metrics & More



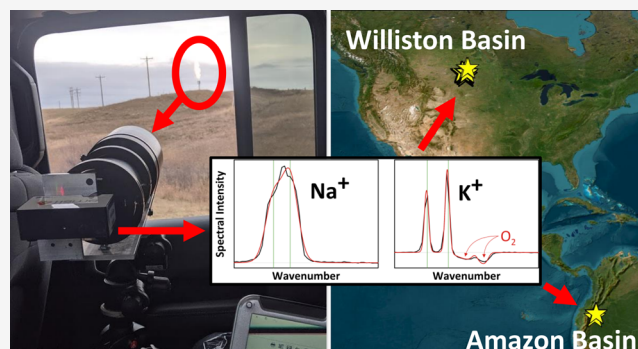
Article Recommendations



Supporting Information

**ABSTRACT:** Pollutant emissions from gas flares in the upstream oil and gas (UOG) industry can be exacerbated by aerosols of coproduced liquid hydrocarbons and formation water that survive separation and enter the flare. Of noteworthy concern is the potential impact of salt-laden aerosols, since the associated chlorine may adversely affect combustion and emissions. Here, we use a novel approach to remotely detect carry-over of salt-laden aerosols into field-operational flares via flame emission spectroscopy targeting two of the most abundant species in produced water samples, sodium and potassium. Ninety-five UOG flares were examined during field campaigns in the Bakken (U.S.A. and Canada) and Amazon (Ecuador) basins. For the first time, carry-over of salt species into flares is definitively detected and further found to be concerningly common, with 74% of studied flares having detectable sodium and/or potassium signatures. Additional analysis reveals that carry-over strongly correlates with reported flared gas volume (positive) and well age (negative), but carry-over was also observed in flares linked to older wells and those flaring relatively little gas. Given the scale of global UOG flaring and the risk of salt-laden aerosols affecting emissions, these findings emphasize the need to review separation standards and re-evaluate pollutant emissions from flares experiencing carry-over.

**KEYWORDS:** Flaring, liquid carry-over, salts, spectrometer, flare emissions, emission spectroscopy, produced water, entrained aerosols



## INTRODUCTION

In the upstream oil and gas (UOG) industry, associated gas that is coproduced with oil is often flared, i.e., combusted in an open-atmosphere turbulent nonpremixed flame. This flaring may be temporary, e.g., during testing or completion of a well, or ongoing, e.g., in oil-producing regions where necessary pipeline infrastructure to capture and transport gas may be lacking. Satellite estimates suggest that more than 90% of all global gas flaring occurs at upstream production sites, totaling 136 billion m<sup>3</sup> of gas in 2022.<sup>1</sup> A primary objective of flaring is to convert potent greenhouse gases in the gas stream (methane and other hydrocarbons) to carbon dioxide, offering a net reduction in the release of climate warming pollutants. However, flare combustion efficiencies are often poor,<sup>2–5</sup> and flares can yield significant emissions of unburned hydrocarbons, oxides of nitrogen and sulfur, carbon monoxide, and black carbon directly to atmosphere.<sup>6–11</sup> Flare pollutants have been linked with various risks to human health and the environment,<sup>12–20</sup> and since the decision to flare is largely based on economical arguments, flaring has garnered attention as an easily mitigatable oil and gas activity.<sup>21</sup>

Flare emissions are sensitive to myriad parameters including wind speed, gas composition, and exit velocity.<sup>2,4,9,22</sup> However, especially at upstream production sites where flare gas must

typically be separated from a produced multiphase mixture of oil, water, and gas, there is a potential to exacerbate emissions via the entrainment of liquid aerosols into the flare stream. Limited field measurements suggest potential for liquid hydrocarbons to reduce flare efficiency,<sup>8</sup> but of greater concern is the entrainment of nonhydrocarbon aerosols (i.e., droplets of formation water high in dissolved solids or flowback fluids related to hydraulic fracturing). Recent studies<sup>23–26</sup> suggest that nonhydrocarbon liquid carry-over has potential to severely augment flare emissions, including experiments by Roth<sup>27</sup> that suggest entrained salt water-based aerosols of typical field salinity could increase the yields of flare pollutants such as benzene, carbon monoxide, and black carbon by up to 9×, 40×, and 3×, respectively, compared to a dry flame without entrained aerosols or a flame with fresh water aerosols. However, despite anecdotal information suggesting liquid carry-over may be common in the field especially during the

**Received:** August 26, 2023

**Revised:** September 28, 2023

**Accepted:** September 29, 2023

**Published:** October 5, 2023



completion and early production stages of a well's lifecycle, to the authors' knowledge, there are no published studies regarding the degree or frequency with which liquid carry-over occurs in practice.

The key objectives of this study were (i) to develop a technique for remotely detecting the presence of nonhydrocarbon aerosols in flare flames via atomic emission spectroscopy, (ii) to deploy this technique in an attempt to prove whether nonhydrocarbon aerosols are indeed carried into flare systems in practice, and (iii) to estimate the prevalence of detected liquid carry-over seen in field campaigns at active upstream production sites. This new technique was deployed in fence-line monitoring of flares at active UOG facilities across two basins in North and South America. Results strongly suggest that liquid carry-over at UOG facilities is common and support further analysis to investigate operational factors that might predict its likelihood.

### THE POTENTIAL FOR LIQUID CARRY-OVER INTO FLARE SYSTEMS

Flare systems at UOG facilities can be vulnerable to liquid carry-over when on-site separation equipment is undersized or does not effectively remove produced liquids such as crude oil, formation water, and hydraulic fracturing fluids from the flare gas stream. Especially in the early production stage of a well's lifecycle, production volumes are generally higher<sup>28,29</sup> leading to higher flow velocities and turbulence levels that can favor the entrainment of liquid aerosols in the gas phase of the multiphase flow. These conditions may preclude gravity settling, a commonly used separation technique,<sup>30</sup> from effectively removing entrained aerosols from the gas stream. Moreover, if surfactants are present in the flowback fluids, foam may develop in the separator vessel requiring operational adjustments that consequently reduce separator efficiency and lead to liquid carry-over.<sup>30</sup> This is especially likely at hydraulically fractured wells where injected fluids containing surfactants and other chemicals can promote foam production.<sup>28,30</sup>

Liquid carry-over at UOG facilities is partially addressed by ANSI/API Standard 521,<sup>31</sup> which provides guidance for designing on-site separation equipment and flare systems in North America and is arguably the most influential resource pertaining to liquid carry-over at oil and gas facilities globally.<sup>32</sup> This standard emphasizes the importance of achieving maximum liquid–gas disengagement because flares are typically not designed to efficiently combust droplets of liquid hydrocarbons.<sup>31</sup> Their recommendation is that on-site separation tanks be sized to remove droplets 300–600  $\mu\text{m}$  in diameter from the gas stream, warning of such consequences as excessive smoking due to incomplete combustion, possible “burning rain”, and flame out.<sup>31</sup> However, this standard is focused primarily on safety concerns rather than emissions and does not address the potential for nonhydrocarbon aerosols to augment flare emissions. Notably, even with properly sized and efficiently operating separators to meet API recommendations, there is presumably potential for the entrainment of aerosols smaller than 300  $\mu\text{m}$ .

Except during the initial flowback phase of a hydraulically fractured well, where fracturing fluids may also be present, nonhydrocarbon aerosols originate from produced water. In regions like North Dakota, produced water is often the majority component in the production stream at UOG facilities.<sup>33</sup> After initial flowback, nonhydrocarbon aerosols

that become entrained into flare systems are expected to match the composition of produced water, which is typically salty with a high concentration of dissolved solids. Figure 1 plots the

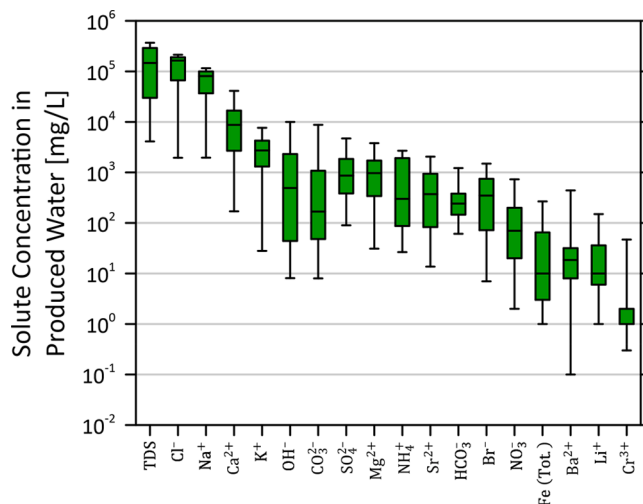


**Figure 1.** Box and whisker plot showing concentrations of the most common solutes in produced water samples from the Williston basin<sup>34</sup> on a logarithmic scale. The boxes identify the median value and extend across the quartiles, while the whiskers span the 90% reference range of the data. TDS = total dissolved solids; Fe (Tot.) = total iron.

concentrations of solutes in produced water samples from UOG facilities in the Williston basin of North Dakota.<sup>34</sup> Noting the logarithmic scale on the vertical axis, chlorine ( $\text{Cl}^-$ ) and sodium ( $\text{Na}^+$ ) ions are the dominant solutes, with average concentrations an order of magnitude greater than those of the next most abundant ions, calcium ( $\text{Ca}^{2+}$ ) and potassium ( $\text{K}^+$ ). The large concentrations of  $\text{Cl}^-$  and  $\text{Na}^+$  suggest that if produced water aerosols were carried into a flare system, these species have the greatest potential to affect emissions. However, of the top four species, sodium and potassium are the best suited for remote optical detection.

Sodium and potassium ions are optically active in the visible spectrum, each having (among other features) persistent doublets, located at 589.00 and 589.59 nm (16,978.07 and 16,960.87  $\text{cm}^{-1}$ ) for sodium's “D-lines” and 766.49 and 769.90 nm (13,046.49 and 12,988.76  $\text{cm}^{-1}$ ) for potassium.<sup>35</sup> Flame emission spectroscopy<sup>36–38</sup> approaches can thus be used to detect the presence of these ions within high-temperature flames. Notwithstanding practical challenges in the field, this suggests that visible spectroscopy of in-field flare flames can theoretically be used to detect the occurrence of liquid carry-over.

### METHODS AND MATERIALS

**Spectrometer System.** Two field-deployable spectrometer systems were developed to remotely inspect visible-spectrum radiative emission from flare flames from outside the fence lines of UOG facilities. A narrowband (437–619 nm) and a broadband (430–1100 nm) spectrometer were selected to isolate the spectra near sodium's D-lines and the potassium doublet, respectively. Referring to further detail in the Supporting Information (SI Section S1), each system employed a 100 mm diameter plano-convex lens of 400 mm focal length to enable the optics to be filled with radiation from

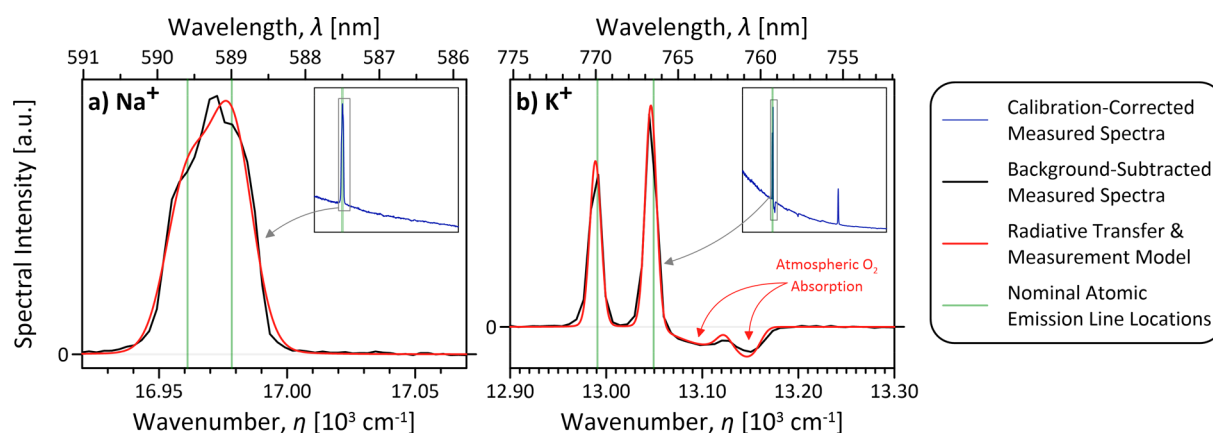


**Figure 2.** Example spectra confirming the detection of (a) sodium and (b) potassium ions in flare flames. Raw measurement data are shown in the inset plots (blue), which were processed to account for dark shot noise and relative intensity calibration as described in the [Methods and Materials](#) section, providing in black the isolated atomic emission signatures and atmospheric absorption by oxygen. The radiative transfer models fitted to each spectrum are shown in red.

the flame, even from the fence-line of surveyed facilities. Captured light was directed onto the entrance aperture (1 mm tall rectangular slit) of each spectrometer (Ocean Insight model Flame-S), dispersed by the diffraction grating, and detected by a 2048-pixel linear charge-coupled device. Slit widths were chosen to balance spectral resolution and field-of-view requirements. A 50- $\mu\text{m}$  wide slit was used with the narrowband spectrometer, and 25- and 10- $\mu\text{m}$  wide slits were used with the broadband spectrometer. Typical full-width half-maximum resolutions were on the order of 18–34  $\text{cm}^{-1}$  for all configurations. Relative intensity calibrations were performed for each spectrometer-slit pairing using an integrating sphere and NIST traceable lamp as detailed by Milani.<sup>39</sup>

**Field Measurement Campaigns.** Field measurements to identify the presence of salt-laden aerosols in UOG sector flare flames were completed during two separate measurement campaigns. The first campaign was performed during November 8–12, 2019 in the Williston Basin's Bakken formation of northwestern North Dakota, U.S.A., and southeastern Saskatchewan, Canada. Eighty-one flares were measured, including 76 in North Dakota and 5 in Saskatchewan. An additional 14 flares were measured during January 30–February 6, 2020, in the Amazon basin of Ecuador near the cities of Nueva Loja (6) and Puerto Francisco de Orellana (8). Between  $10^3$  and  $10^5$  radiative intensity spectra, corresponding to up to 25 min of sampling, were acquired at high temporal frequency (approximately 110 Hz on average) for each flare and analyzed for the atomic emission signatures of sodium and potassium.

**Spectral Analysis.** Narrowband and broadband spectra of field-operational flares were analyzed to identify potential emission signatures of sodium and potassium ions. The algorithmic procedure is summarized in detail in [SI Section S3](#). Briefly, the analysis begins with a basic preprocessing procedure ([SI Section S3.1](#)) that (1) subtracts dark shot noise from the acquired spectra, (2) crops the spectra to a wavelength range of interest, (3) scales the raw data via the relative spectral response calibrations, and (4) resamples the spectral intensity from a wavelength domain (i.e., units of  $\text{W}/(\text{sr}\cdot\text{m}^2\cdot\text{nm})$ ) to a wavenumber/energy (units of  $\text{W}/(\text{sr}\cdot\text{m}^2\cdot\text{cm}^{-1})$ ) domain. At this point, measured spectral intensity data resemble blackbody emission due to soot incandescence in the flare flame with any additional emission signatures of sodium

and potassium, which are attenuated by the atmosphere and smoothed by the diffraction-limited optics. These phenomena are captured by a radiative transfer and measurement model (RTMM; described in [SI Section S3.2](#)).

The analysis continues by masking spectra where any emission or absorption signatures are expected (see [SI Table S1](#)) and fitting a simplified RTMM ([SI Section S3.3](#)) to the surviving data. This serves two purposes. First, a goodness-of-fit test confirms that radiation from the flame filled each spectrometer's optics, identifying measured spectra for removal if sky radiation were potentially superimposed on the spectra. Second, the fitted temperature of the blackbody distribution can be interpreted as an effective flame temperature that is later used to model radiative emission from the flame. Afterward, potential signatures of sodium and potassium are isolated by subtracting blackbody emission from the measured spectra via locally weighted smoothing (LOESS<sup>40</sup>) of the masked data.

Finally, the RTMM considering atomic emission by sodium and potassium at the inferred flame temperature, absorption by the atmosphere, and optical properties of the spectrometers ([SI Section S3.4](#)) is fit to the isolated spectra. This model includes optimized parameters that account for the relative intensity of the signal, spectral resolution of the spectrometers, and spectral shift resulting from asymmetrical filling of the optics. Optimized parameters and measurement data for each spectrum surviving earlier quality control are used to objectively test for detectable sodium or potassium signature(s) via multiple criteria detailed in [SI Section S3.5](#).

## RESULTS AND DISCUSSION

### Detection of Liquid Carry-Over into Flare Systems.

[Figure 2](#) plots example spectra obtained from an operating flare in North Dakota, U.S.A., using the narrowband spectrometer for sodium detection ([Figure 2a](#)) and broadband spectrometer for potassium detection ([Figure 2b](#)). The insets of the figures show the calibration-corrected spectra measured in the field, which are the superposition of blackbody emission by soot, atomic emission by sodium/potassium, and atmospheric absorption. Removal of the blackbody background from the signal provides the isolated effect of atomic emission and atmospheric absorption, as shown by the black lines in the figures. Least squares fitting of the RTMM to the isolated



spectra are shown in red, illustrating tight alignment with measured spectra. The measurement spectra of Figure 2 conclusively identify the presence of sodium and potassium in the example flare flame. In the absence of other mechanisms for these elements to enter a flare gas stream, this observation represents the first definitive evidence of liquid carry-over into UOG flares.

The spectral analysis was applied to all measurement data to elucidate the prevalence of liquid carry-over in upstream oil and gas flares. As detailed in SI Section S3.5, an algorithm was developed to inspect the optimized RTMM for the measured spectra. This algorithm evaluated both the peak value of background-subtracted measurement data against instrument noise and the goodness-of-fit of the RTMM to identify spectra with statistically significant sodium and/or potassium signatures. Spectra for each flare were also manually reviewed.

**Prevalence of Nonhydrocarbon Liquid Carry-Over in Two Different Basins.** Figure 3 summarizes the proportion

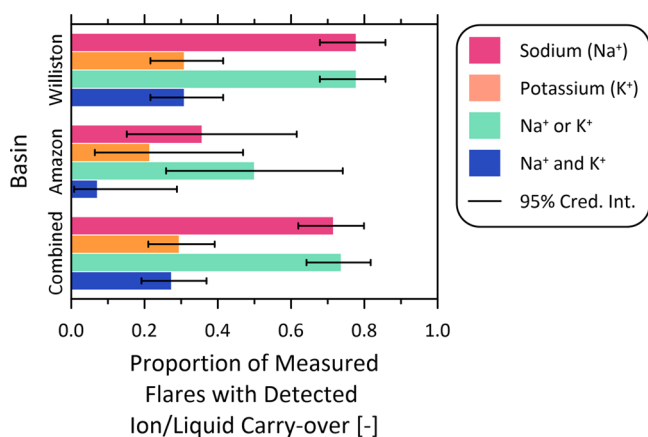


**Figure 3.** Rates of detection of sodium and/or potassium ions in flare flames in the Williston and Amazon basins and for the combined sample set. Error bars indicate the 95% credible interval for the true occurrence rate. See SI Table S2 for the numerical values of these results and additional results also parsed by subregion in each basin.

of studied flares with detected liquid carry-over. Nearly three-quarters (74%) of all measured flares had detectable signatures

of sodium or potassium. There were slight differences across the study regions, with liquid carry-over being more prevalent in the Williston basin than in Ecuador, although 95% credible intervals estimated using the noninformative Jeffreys' prior<sup>41</sup> slightly overlap. All 63 detections in the Williston basin had detectable sodium signatures, with 25 also having detectable potassium. This observation is consistent with the relative prevalence of sodium in formation water in the Williston basin (>22× more sodium than potassium as per Figure 1) and implies carry-over of formation water, specifically. Referring also to Figure S2 of the SI, the detected liquid carry-over in the Williston basin (63 of 81 flares) followed no particular spatial pattern. By contrast, recognizing that the sample size is small, the two regions of Ecuador were notably different with 6 of 6 (100%) and 1 of 8 (12.5%) flares having detectable liquid carry-over in the Nueva Loja and Puerto Francisco de Orellana regions, respectively. Furthermore, one flare in Ecuador had only detectable potassium. Basin-level variation of detectable carry-over suggests that it may vary with location, where factors including well production volumes, separation infrastructure, and formation water composition may impact spatial variability.

**Potential Drivers of Liquid Carry-Over and Implications.** Public production and completion data,<sup>42</sup> available for the wells feeding 66 of the studied flares in North Dakota, were used to identify parameters influencing liquid carry-over at UOG flares. A two-sample Welch's *t* test was employed to compare the means of available production parameters aggregated over corresponding wells for the subsets of flares with and without detected carry-over. The analysis considered the average time since well completion (TSC); total oil, gas, or water production; and total reported flaring. Figure 4 plots the results of this hypothesis test for (a) TSC and (b) flared volume; SI Figure S3 plots results for the remaining parameters. Means of both TSC and flared volume were statistically different at 5% significance for flares with and without detected carry-over. Wells connected to flares with detected carry-over were generally completed more recently (616 days on-average), which is likely explained in part by declining gas production/flaring as wells age. Indeed, the hypothesis testing suggests that flared volume was the stronger correlate (Figure 4b), with higher monthly flared volumes

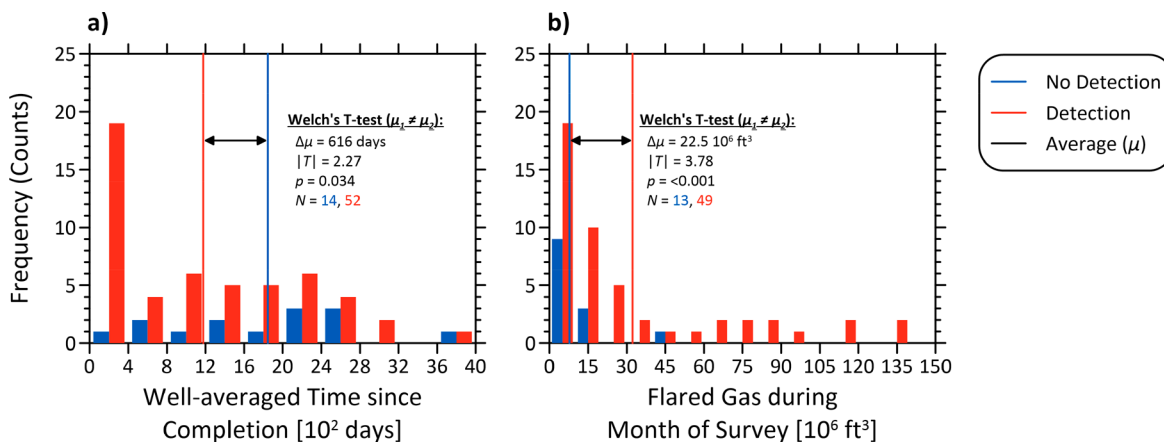


**Figure 4.** Distribution of studied flares with and without detected liquid-carry over as a function of (a) time since well completion and (b) flared gas volume. Vertical lines indicate the means in each subsample. Although there are instances of flares with and without detected carry-over across the distribution of well ages and flared gas rates, Welch's *t* tests suggest a statistically significant difference between the samples such that flares associated with younger wells and more gas production/flaring are more likely to exhibit liquid carry-over.

implying liquid carry-over is more likely. This is understandable given the known reduction in separator efficiency at high gas flow rates. However, it is also notable that liquid carry-over was still detected at flares linked to wells older than five years and producing and flaring relatively little gas. Further modeling (see SI Section S4.3) considering combinations of available production parameters via binomial regression<sup>43</sup> showed negligible improvement in predicting liquid carry-over versus a simpler flare volume model, which suggests that other nonmodeled and unknown factors (e.g., separator design, liquid level within the separator) are likely also important. Thus, despite the statistical significance of these tests shown in Figure 4, in practice carry-over appears to be pervasive across wells of all ages and gas production and flaring rates.

The apparent pervasiveness of liquid carry-over in flare flames is concerning due to its potential implications for emissions. Beyond exacerbating production of unwanted hazardous species like carbon monoxide and benzene,<sup>27</sup> the introduction of salt-bound chlorine to hydrocarbon flames raises the potential for forming chlorinated hydrocarbons.<sup>44–47</sup> While the present results speak directly only to the detected presence of salt species in flare flames, the high frequency of detection in the field coupled with analysis demonstrating that carry-over can occur throughout the lifetime of a well suggests an urgent need for studies assessing impacts on in-field flare emissions. Furthermore, caution may be warranted if applying emission factors derived from measurements or tests on nonproduction flares (where liquid carry-over is not expected to occur) to upstream flares. In parallel, operators of flares and regulators of flaring would be wise to revisit specifications and targeted efficiencies of separators so that the propensity for carry-over of nonhydrocarbon species into flare systems can be reduced or simply avoided. Finally, success of the developed diagnostic, assembled from readily purchasable components, in detecting spectral signatures of salt species in flare flames offers a simple way to remotely monitor and verify the effectiveness of flare gas separation systems in the field.

## ■ ASSOCIATED CONTENT

### Data Availability Statement

A summary table of flare-by-flare detection results and estimated persistence is available through the Carleton University dataverse at <https://doi.org/10.5683/SP3/LAYJFW>.

### SI Supporting Information

The Supporting Information is available free of charge at <https://pubs.acs.org/doi/10.1021/acs.estlett.3c00613>.

Details of the spectrometer systems; maps of the field campaigns indicating positive and null detections; details of the spectral data processing and radiative transfer and measurement model (RTMM); and statistical analysis of liquid carry-over detection results with additional references (PDF)

## ■ AUTHOR INFORMATION

### Corresponding Author

**Matthew R. Johnson** – Energy and Emissions Research Laboratory, Department of Mechanical and Aerospace Engineering, Carleton University, Ottawa, ON, Canada K1S 5B6; [orcid.org/0000-0002-3637-9919](https://orcid.org/0000-0002-3637-9919); Email: [Matthew.Johnson@carleton.ca](mailto:Matthew.Johnson@carleton.ca)

## Authors

**Zachary R. Milani** – Energy and Emissions Research Laboratory, Department of Mechanical and Aerospace Engineering, Carleton University, Ottawa, ON, Canada K1S 5B6

**Bradley M. Conrad** – Energy and Emissions Research Laboratory, Department of Mechanical and Aerospace Engineering, Carleton University, Ottawa, ON, Canada K1S 5B6; [orcid.org/0000-0003-3678-7434](https://orcid.org/0000-0003-3678-7434)

**Cameron S. Roth** – Energy and Emissions Research Laboratory, Department of Mechanical and Aerospace Engineering, Carleton University, Ottawa, ON, Canada K1S 5B6

Complete contact information is available at:

<https://pubs.acs.org/10.1021/acs.estlett.3c00613>

## Author Contributions

Conceptualization: Z.R.M. and M.R.J. Investigation: Z.R.M., C.S.R., and M.R.J. Data curation: Z.R.M. Methodology, software, validation, and formal analysis: Z.R.M. and B.M.C. Writing – Original draft: Z.R.M., B.M.C., and M.R.J. Writing – Review & Editing: All authors. Supervision and funding acquisition: M.R.J.

## Notes

The authors declare no competing financial interest.

## ■ ACKNOWLEDGMENTS

This work was completed as part of the FlareNet strategic network supported by the Natural Sciences and Engineering Research Council (NSERC; Grant Nos. 479641, 06632, and 522658) of Canada, the World Bank Global Gas Flaring Reduction (GGFR) partnership (project manager Francisco Sucre), and Natural Resources Canada (project manager: Michael Layer; Grant No. CH-GHG IETS-19-103). We are especially grateful for the support of Petroamazonas and local support personnel including Javier Villacis and David Neira in coordinating field measurements in Ecuador as part of a larger effort to quantify and mitigate flaring in the region.

## ■ REFERENCES

- (1) EOG. *Global Gas Flaring Observed from Space*. [https://eogdata.mines.edu/products/vnf/global\\_gas\\_flare.html](https://eogdata.mines.edu/products/vnf/global_gas_flare.html) (accessed 2023–06–12).
- (2) Johnson, M. R.; Kostiuk, L. W. A Parametric Model for the Efficiency of a Flare in Crosswind. *Proc. Combust. Inst.* **2002**, *29* (2), 1943–1950.
- (3) Plant, G.; Kort, E. A.; Brandt, A. R.; Chen, Y.; Fordice, G.; Gorchoy Negron, A. M.; Schwietzke, S.; Smith, M.; Zavala-Araiza, D. Inefficient and Unlit Natural Gas Flares Both Emit Large Quantities of Methane. *Science* (80-). **2022**, *377* (6614), 1566–1571.
- (4) Burt, D. C.; Corbin, D. J.; Armitage, J. R.; Crosland, B. M.; Jefferson, A. M.; Kopp, G. A.; Kostiuk, L. W.; Johnson, M. R. A Methodology for Quantifying Combustion Efficiencies and Species Emission Rates of Flares Subjected to Crosswind. *J. Energy Inst.* **2022**, *104*, 124–132.
- (5) Gvakharia, A.; Kort, E. A.; Brandt, A. R.; Peischl, J.; Ryerson, T. B.; Schwarz, J. P.; Smith, M. L.; Sweeney, C. Methane, Black Carbon, and Ethane Emissions from Natural Gas Flares in the Bakken Shale, North Dakota. *Environ. Sci. Technol.* **2017**, *51* (9), 5317–5325.
- (6) Torres, V. M.; Herndon, S. C.; Wood, E.; Al-Fadhli, F. M.; Allen, D. T. Emissions of Nitrogen Oxides from Flares Operating at Low Flow Conditions. *Ind. Eng. Chem. Res.* **2012**, *51* (39), 12600–12605.
- (7) Knighton, W. B.; Herndon, S. C.; Franklin, J. F.; Wood, E. C.; Wormhoudt, J.; Brooks, W.; Fortner, E. C.; Allen, D. T. Direct

Measurement of Volatile Organic Compound Emissions from Industrial Flares Using Real-Time Online Techniques: Proton Transfer Reaction Mass Spectrometry and Tunable Infrared Laser Differential Absorption Spectroscopy. *Ind. Eng. Chem. Res.* **2012**, *51* (39), 12674–12684.

(8) Strosher, M. T. Characterization of Emissions from Diffusion Flare Systems. *J. Air Waste Manage. Assoc.* **2000**, *50* (10), 1723–1733.

(9) Johnson, M. R.; Kostiuk, L. W. Efficiencies of Low-Momentum Jet Diffusion Flames in Crosswinds. *Combust. Flame* **2000**, *123* (1–2), 189–200.

(10) Johnson, M. R.; Wilson, D. J.; Kostiuk, L. W. A Fuel Stripping Mechanism for Wake-Stabilized Jet Diffusion Flames in Crossflow. *Combust. Sci. Technol.* **2001**, *169* (1), 155–174.

(11) Conrad, B. M.; Johnson, M. R. Field Measurements of Black Carbon Yields from Gas Flaring. *Environ. Sci. Technol.* **2017**, *51* (3), 1893–1900.

(12) Anejionu, O. C. D.; Whyatt, J. D.; Blackburn, G. A.; Price, C. S. Contributions of Gas Flaring to a Global Air Pollution Hotspot: Spatial and Temporal Variations, Impacts and Alleviation. *Atmos. Environ.* **2015**, *118*, 184–193.

(13) Motte, J.; Alvarenga, R. A. F.; Thybaut, J. W.; Dewulf, J. Quantification of the Global and Regional Impacts of Gas Flaring on Human Health via Spatial Differentiation. *Environ. Pollut.* **2021**, *291*, 118213.

(14) Willis, M.; Hystad, P.; Denham, A.; Hill, E. Natural Gas Development, Flaring Practices and Paediatric Asthma Hospitalizations in Texas. *Int. J. Epidemiol.* **2021**, *49* (6), 1883–1896.

(15) Blundell, W.; Kokoza, A. Natural Gas Flaring, Respiratory Health, and Distributional Effects. *J. Public Econ.* **2022**, *208*, 104601.

(16) Nwosisi, M. C.; Oguntoke, O.; Taiwo, A. M.; Agbozu, I. E.; Noragbon, E. J. Spatial Patterns of Gas Flaring Stations and the Risk to the Respiratory and Dermal Health of Residents of the Niger Delta, Nigeria. *Sci. African* **2021**, *12*, No. e00762.

(17) Chen, C.; McCabe, D. C.; Fleischman, L. E.; Cohan, D. S. Black Carbon Emissions and Associated Health Impacts of Gas Flaring in the United States. *Atmosphere (Basel)*. **2022**, *13* (3), 385.

(18) Sand, M.; Berntsen, T. K.; Von Salzen, K.; Flanner, M. G.; Langner, J.; Victor, D. G. Response of Arctic Temperature to Changes in Emissions of Short-Lived Climate Forcers. *Nat. Clim. Chang.* **2016**, *6* (3), 286–289.

(19) Böttcher, K.; Paunu, V.-V.; Kupiainen, K.; Zhizhin, M.; Matveev, A.; Savolahti, M.; Klimont, Z.; Väätäinen, S.; Lamberg, H.; Karvosenoja, N. Black Carbon Emissions from Flaring in Russia in the Period 2012–2017. *Atmos. Environ.* **2021**, *254* (March), 118390.

(20) Stohl, A.; Klimont, Z.; Eckhardt, S.; Kupiainen, K.; Shevchenko, V. P.; Kopeikin, V. M.; Novigatsky, A. N. Black Carbon in the Arctic: The Underestimated Role of Gas Flaring and Residential Combustion Emissions. *Atmos. Chem. Phys.* **2013**, *13* (17), 8833–8855.

(21) The World Bank Group. *Global Gas Flaring Reduction Partnership*. <https://www.worldbank.org/en/programs/gasflaringreduction#1> (accessed 2023–08–09).

(22) Torres, V. M.; Herndon, S. C.; Allen, D. T. Industrial Flare Performance at Low Flow Conditions. 2. Steam- and Air-Assisted Flares. *Ind. Eng. Chem. Res.* **2012**, *51* (39), 12569–12576.

(23) Jefferson, A. M. *Exploratory Experiments to Determine Effects of Injected Aerosolized Water, Hydrochloric Acid, and Sodium Chloride Solutions on Lab-Scale Flare Emissions*. Master's Thesis, Carleton University, Ottawa, Ontario, 2017. DOI: 10.22215/etd/2017-11970.

(24) Kazemimanesh, M. *Effects of Non-Hydrocarbon Liquids on Particulate Emissions of Flares*. Master's Thesis, University of Alberta, 2014.

(25) Kazemimanesh, M.; Dastanpour, R.; Baldelli, A.; Moallemi, A.; Thomson, K. A.; Jefferson, M. A.; Johnson, M. R.; Rogak, S. N.; Olfert, J. S. Size, Effective Density, Morphology, and Nano-Structure of Soot Particles Generated from Buoyant Turbulent Diffusion Flames. *J. Aerosol Sci.* **2019**, *132*, 22–31.

(26) Trivanovic, U.; Baldelli, A.; Kazemimanesh, M.; Conrad, B. M.; Jefferson, A. M.; Corbin, J. C.; Johnson, M. R.; Olfert, J. S.; Rogak, S. N. The Effect of Inorganic Salts from Flowback Operations on the

Size, Effective Density, Mixing State, and Optical Properties of Soot from Gas Flares. In *Combustion Institute Canadian Section Spring Technical Meeting*; Kelowna, BC, 2019; p 6.

(27) Roth, C. *Gas- and Particulate-Phase Emissions from Lab-Scale Flares Experiencing Liquid Carryover*. Master's Thesis, Carleton University, Ottawa, Ontario, 2022. DOI: 10.22215/etd/2022-15013.

(28) Bai, B.; Goodwin, S.; Carlson, K. Modeling of Frac Flowback and Produced Water Volume from Wattenberg Oil and Gas Field. *J. Pet. Sci. Eng.* **2013**, *108*, 383–392.

(29) Höök, M.; Davidsson, S.; Johansson, S.; Tang, X. Decline and Depletion Rates of Oil Production: A Comprehensive Investigation. *Philos. Trans. R. Soc. A Math. Phys. Eng. Sci.* **2014**, *372* (2006), 20120448.

(30) Shaban, H. I. A Study of Foaming and Carry-over Problems in Oil and Gas Separators. *Gas Sep. Purif.* **1995**, *9* (2), 81–86.

(31) API. *API Standard 521: Pressure-Relieving and Depressuring Systems*; American Petroleum Institute (API), 2014. <https://www.api.org/products-and-services/standards/important-standards-announcements/standard521>.

(32) API. *API Standards: International Usage and Deployment*; American Petroleum Institute (API), 2022. <https://www.api.org/-/media/APIWebsite/products-and-services/apiinternationalstandardsreport.pdf>.

(33) Veil, J. *U.S. Produced Water Volumes and Management Practices in 2017*; Ground Water Research and Education Foundation, 2020. [https://www.gwpc.org/wp-content/uploads/2020/02/pw\\_report\\_2017\\_final.pdf](https://www.gwpc.org/wp-content/uploads/2020/02/pw_report_2017_final.pdf) (accessed 2023–09–23).

(34) Blondes, M. S.; Gans, K. D.; Engle, M. A.; Kharaka, Y. K.; Reidy, M. E.; Saraswathula, V.; Thordsen, J. J.; Rowan, E. L.; Morrissey, E. A. *U.S. Geological Survey National Produced Waters Geochemical Database (Ver. 2.3, January 2018)*; U.S. Geological Survey, 2018.

(35) Kramida, A.; Ralchenko, Y.; Reader, J. *Atomic Spectra Database (version 5.8)*; NIST, DOI: 10.18434/T4W30F.

(36) Alkemade, C. T. J.; Bleekrode, R.; Burger, J. C.; Butler, C. C.; Cath, P. G.; Fassel, V. A.; Gilbert, P. T.; Gillies, W.; Herrmann, R.; Kniseley, R. N.; Mavrodineanu, R.; Menis, O.; Müller-Herget, W.; Pinta, M.; Rains, T. C.; Smith, R.; Willis, J. B.; Winefordner, J. D.; Yamasaki, G. K. *Analytical Flame Spectroscopy*; Mavrodineanu, R., Ed.; Macmillan Education UK: London, 1970; Vol. 52. DOI: 10.1007/978-1-349-01008-0.

(37) Gibson, J. H.; Grossman, W. E. L.; Cooke, W. D. Excitation Processes in Flame Spectrometry. *Anal. Chem.* **1963**, *35* (3), 266–277.

(38) Gaydon, A. G. *The Spectroscopy of Flames*; Springer Dordrecht: Dordrecht, 1974. DOI: 10.1007/978-94-009-5720-6.

(39) Milani, Z. *Remote Detection of Sodium and Potassium Atomic Emission Signatures as an Indicator of Liquid Carry-Over into Flare Systems*. Master's Thesis, Carleton University, Ottawa, Ontario, 2021. DOI: 10.22215/etd/2021-14762.

(40) Cleveland, W. S.; Devlin, S. J. Locally Weighted Regression: An Approach to Regression Analysis by Local Fitting. *J. Am. Stat. Assoc.* **1988**, *83* (403), 596–610.

(41) Jeffreys, H. *Theory of Probability*, 3rd ed.; Clarendon Press: Oxford, UK, 1961.

(42) North Dakota Industrial Commission Oil and Gas Division. *Well Index*. <https://www.dmr.nd.gov/oilgas/basicservice.asp> (accessed 2021–04–15).

(43) Conrad, B. M.; Tyner, D. R.; Johnson, M. R. Robust Probabilities of Detection and Quantification Uncertainty for Aerial Methane Detection: Examples for Three Airborne Technologies. *Remote Sens. Environ.* **2023**, *288*, 113499.

(44) Wikström, E.; Ryan, S.; Touati, A.; Tabor, D.; Gullett, B. K. Origin of Carbon in Polychlorinated Dioxins and Furans Formed during Sooting Combustion. *Environ. Sci. Technol.* **2004**, *38* (13), 3778–3784.

(45) Stanmore, B. R. The Formation of Dioxins in Combustion Systems. *Combust. Flame* **2004**, *136* (3), 398–427.

- (46) Altarawneh, M.; Dlugogorski, B. Z.; Kennedy, E. M.; Mackie, J. C. Mechanisms for Formation, Chlorination, Dechlorination and Destruction of Polychlorinated Dibenzo-p-Dioxins and Dibenzofurans (PCDD/Fs). *Prog. Energy Combust. Sci.* **2009**, *35* (3), 245–274.
- (47) Bumb, R. R.; Crummett, W. B.; Cutie, S. S.; Gledhill, J. R.; Hummel, R. H.; Kagel, R. O.; Lamparski, L. L.; Luoma, E. V.; Miller, D. L.; Nestruck, T. J.; Shadoff, L.; Stehl, R. H.; Woods, J. S. Trace Chemistries of Fire: A Source of Chlorinated Dioxins. *Science* (80-). **1980**, *210* (4468), 385–390.